Published by
NIGERIAN SOCIETY OF PHYSICAL SCIENCES
Available online @ https://journal.nsps.org.ng/index.php/jnsps

J. Nig. Soc. Phys. Sci. 6 (2024) 1830

Journal of the Nigerian Society of Physical Sciences

The analysis of a novel COVID-19 model with the fractional-order incorporating the impact of the vaccination campaign in Nigeria via the Laplace-Adomian Decomposition Method

Akeem Olarewaju Yunus[a,b], Morufu Oyedunsi Olayiwola[a,*]

[a]*Department of Mathematical Sciences, Osun State University, Osogbo, Nigeria*
[b]*Department of Mathematics and Statistics, Osun State College of Technology, Esa-Oke, Nigeria*

Abstract

This study underscores the crucial role of COVID-19 vaccinations in managing the pandemic, with a specific focus on Nigeria. Employing a fractional-order mathematical modeling approach, the research assesses vaccination efficacy, minimum effectiveness, and duration. The model's numerical solution is derived through the Laplace Adomian Decomposition Method (LADM), utilizing rapidly converging infinite series. Simulation results illustrate the impact of COVID-19 transmission and vaccination rates. The study concludes that implementing a vaccination strategy in an integer order proves to be the most effective approach to controlling the spread of COVID-19. These findings have significant implications for researchers, policymakers, and healthcare workers. They emphasize the central role of fractional calculus in facilitating vaccine implementation in the ongoing battle against COVID-19. The study calls for global efforts to maximize vaccination implementation for the overall benefit of public health.

DOI:10.46481/jnsps.2024.1830

Keywords: Caputo fractional derivative, COVID-19 disease, Laplace-Adomian decomposition method, Vaccination rate

Article History :
Received: 23 October 2023
Received in revised form: 25 January 2024
Accepted for publication: 25 February 2024
Published: 27 March 2024

Communicated by: T. Latunde

1. Introduction

Nigeria was completely affected by the COVID-19 epidemic. As it has in many countries around the world, the virus is continuing to spread and disrupt daily life [1–4]. One of the most effective strategies to combat the spread of the virus and mitigate its societal effects is vaccination. However, Nigeria has faced several challenges in implementing its vaccination program, including issues related to its healthcare infrastructure, vaccine hesitancy, and the spread of misinformation. Despite these hurdles, the African Union has secured vaccine supplies for the continent through initiatives like the Nigeria Vaccine Acquisition Trust, and vaccination efforts are gaining momentum.

The COVID-19 vaccine has played a crucial role in Nigeria by significantly reducing the incidence of severe illness, hos-

*Corresponding author: Tel.: +234-813-110-9234
Email address: olayiwola.oyedunsi@uniosun.edu.ng (Morufu Oyedunsi Olayiwola)

pitalizations, and fatalities among those who have received it. Research conducted in Morocco, for example, found that vaccination reduced the risk of mortality by an impressive 91% and lowered the likelihood of hospitalization by 81% [5–7]. Similarly, studies in South Africa revealed that immunization led to an 80% reduction in hospitalization and a 60% decrease in mortality [8–11]. Given these amazing results, it is critical to investigate the impact of the COVID-19 epidemic on Nigeria further. In light of the present epidemic, this study aims to analyze the medical advantages of keeping up regular vaccinations among young people in Nigeria. We specifically want to assess the chance of obtaining a severe acute respiratory syndrome coronavirus 2 (SARS-CoV-2) infection when attending routine vaccination treatment locations, taking into account both high- and low-impact scenarios. Nigeria has been devastated by the COVID-19 epidemic. Drawing from successful vaccination strategies in other countries, such as Israel, which achieved a rapid rollout of vaccines with impressive coverage rates [12], we aim to provide insights that can inform Nigeria's ongoing efforts. Additionally, it is important to recognize that Nigeria faces significant challenges. Nevertheless, several waves of the COVID-19 pandemic have also affected other countries in the geographical region, including Bangladesh, India, Indonesia, Nepal, Malaysia, and Myanmar, frequently with less study emphasizing these experiences.

Understanding the nuances of these different contexts is vital for crafting effective responses and ensuring the health and well-being of all affected populations. The emergence of the Omicron variant has raised concerns about the ongoing COVID-19 pandemic. The study sets the stage for an evaluation of Omicron's effects in six specific regions: South Asia, Southeast Asia, and Oceania. aims to assess the reproduction number and infection fatality rate (IFR) in these areas using a model that accounts for susceptibility, vaccination, exposure, infection, hospitalization, death, and recovery with a variable transmission rate [13, 14]. Omicron's swift spread across these six countries highlights its increased transmissibility and potential for new pandemic waves. As vaccination coverage grows, simulations suggest the Omicron impact may be reduced, lessening severe illness and fatalities [15]. A novel multi-strain SV EAIR epidemic model has been established in the pursuit of understanding and effectively managing the spread of multi-strain infectious diseases [16]. This model extends the traditional susceptible-exposed-infectious-recovered (SEIR) model to account for individuals with natural immunity (N) and those who have been immunized (V), allowing for simulations of disease dynamics involving various strains. These models are essential in predicting the transmission of viral diseases, especially ones where several strains spread concurrently. In addition, COVID-19 vaccination efforts in Nigeria have had a significant positive influence on lowering serious disease, hospitalizations, and deaths while also curbing the virus's spread. However, there remains a pressing need to accelerate vaccination roll out efforts to prevent the emergence of new variants. Collaboration between governments and international organizations is essential to overcome the challenges hindering the vaccination campaign and ensure equitable access to vaccines. Understanding public sentiment towards COVID-19 booster vaccinations is critical to shaping vaccination policies. Research indicates that the acceptance rate of booster shots in Algeria is moderate, with variations among demographic groups, including higher reluctance and acceptance rates among males, individuals over 60, and those with chronic illnesses [17]. These findings underscore the importance of addressing psychological factors related to vaccine efficacy and safety in vaccination promotion efforts. In the realm of epidemiology, fractional-order modeling has gained attention due to its ability to capture complex and nonlinear disease dynamics [18–24]. This approach offers an alternative to conventional integer-order models by considering memory effects, such as immunity among recovered individuals, and varying infection and recovery rates over time [25–27]. The Caputo-Fabrizio model and the Atangana-Baleanu model are two examples of fractional order models that offer understanding of disease dynamics, the effects of vaccines, and healthcare capacity's role in disease spread. However, further research is needed to validate and refine these models for accurate prediction of disease spread.

Mathematical models have become indispensable tools in understanding and predicting the COVID-19 pandemic's behavior. Because of their capacity to take into consideration non-locality and memory effects, fractional-order mathematical models have gained acceptance, assisting in a more exact portrayal of the pandemic's growth [28–32]. In order to simulate the COVID-19 epidemic and inform methods for promoting health, these models have proven to be quite helpful. According to Ref. [33], the article simulates COVID-19 transmission using the Caputo fractional derivative, providing conditions and stability. Laplace Adomian decomposition approximates solutions. The graphical interpretation in Mathematical indicates disease control options through rate modifications, providing insights and practical consequences for management. Nonetheless, the vaccine compartment was not considered. According to Ref. [34], a fractional-order COVID-19 model is analyzed using the combination of the q-homotopy analysis method (q-HAM) and Sumudu transform techniques, incorporating the Liouville-Caputo method for the fractional operator. To assess model equilibrium stability, a numerical analysis using the extended Adams-Bashforth-Moulton approach is performed. Authors According to Ref. [35], using the Caputo fractional-order derivative to examine a COVID-19 mathematical model with lockdown. It proves solution uniqueness, explores equilibrium stability, and uses the residual power series approach to approximate a fractional power series. Theoretical discoveries are validated by numerical and graphical evidence. In mathematical modeling, researchers widely use the Caputo fractional differential operator to characterize disease transmission dynamics, considering memory effects, long-term dependencies, repeated patterns and trends in disease propagation to improves forecast accuracy during numerical simulations [36], However, caution is advised, as highlighted in Ref. [37], regarding the careful selection of the fractional operator and addressing challenges related to non-locality, requiring specialized numerical methods. Ref. [38] illustrates applying the Caputo fractional order in COVID-19 modeling, demonstrating a versatile framework

for analyzing complex dynamics within a population without constraints using high-risk quarantine measures. The effectiveness of Caputo fractional order operators is further emphasized by successful applications in various scenarios, including Lassa fever outbreak modeling [39], tuberculosis modeling [40], and diphtheria transmission [41]. These successes validate our decision to use the Caputo fractional order in our study, providing a more flexible framework for capturing the underlying dynamics that the classical derivative cannot fully capture. Numerical simulation is vital in mathematical modeling, particularly for disease trend forecasting. Before simulation, models are usually solved using semi-analytic or numerical techniques. For example in Refs. [42, 43], the authors utilize compact finite differences and shifted Gegenbauer polynomials for discretizing time derivatives in space fractional order diffusion equations. They extend to shifted Vieta-Lucas polynomials, addressing generalized-fractional integro-differential equations with nonlocal boundary conditions through the Galerkin method. Their findings demonstrate that the closed-form approximate solution converges to the exact solution of the problem. due to inherent nonlinearity. Common methods include the homotopy perturbation method [44] and the Laplace-Adomian decomposition method (LADM) [45], using polynomials to handle nonlinear systems. In fractional differential equations, LADM is preferred for efficiency, using the Laplace transform to convert differential operators into solvable algebraic equations. Existing literature [46] confirms LADM's reliability in describing patterns in immunology and fractional-order epidemic models. Our study adopts LADM to solve a proposed fractional-order COVID-19 model for a reliable approximate solution, facilitating easy parameter adjustment during simulation. In summary, this study uses advanced mathematical modeling, including Caputo's fractional-order derivative analysis, to assess COVID-19 vaccination efficacy in Nigeria. Simulation results show the impact of transmission and vaccination rates, emphasizing the pivotal role of full vaccination. It has global implications for researchers, policymakers, and healthcare workers in the fight against COVID-19.

2. Preliminaries

Some fundamental definition from fractional calculus This section presents essential concepts and definitions from fractional calculus but suggests referring to additional resources for a more comprehensive understanding of the topic.

Definition 1. **Fractional integration** [18]:

$$(J^{\xi}_{t_0} f)(t) = \frac{1}{\Gamma(\xi)} \int (t-w)^{\xi-1} f(w) dw, \xi \geq 0, t \geq t_0.$$

Definition 2 [18]. The gamma function $\Gamma(\xi) = \int_o^{\infty} t^{\xi-1} \ell^{-t} dt$, is continuous for all $\xi \geq 0$.

Definition 3 [18]. The Riemann-Liouville fractional integration of order $\xi \geq 0$ for a real positive function is given by

$$J^{\xi}_t f(t) = \frac{1}{\Gamma(n-\xi)} \left(\frac{d}{dy}\right)^n \int_a^t (t-y)^{n-\xi-1} f(y) dy.$$

Definition 4 [38]. The Laplace transform of function $h(t)$ with order η is defined as $L[h^{\eta}(t)] = \xi^{\eta} L[h(t)] - \xi^{\eta-1} h(0) - \xi^{\eta-2} h'(0) - \xi^{\eta-3} \xi''(0)$.

The inverse Laplace transform of $\frac{h(s)}{s}$ is $L^{-1} \frac{h(s)}{s} = \int_0^t h(t) dt$.

The Laplace transform of $f(t) = t^{\lambda}$ is $L(t^{\lambda}) = \frac{\Gamma(\lambda+1)}{s^{\lambda+1}}$ and the inverse transform is $L^{-1}\left(\frac{1}{s^{\lambda+1}}\right) = \frac{t^{\lambda}}{\Gamma(\lambda+1)}$.

Definition 5 [38]. The Adomian polynomials denoted by $X_0, X_{1,\ldots} X_n$, consists in the decomposition of the unknown function $p(t)$ whose series can be expressed as$p(t) = q_0 + q_1 + q_2 + \cdots q_n$ is given as:

$$X_n = \frac{1}{n} \frac{d^n}{d\lambda^n} \left[H(t) \sum_{j=0}^{n} p_j \lambda^j \right]_{\lambda=0}.$$

3. Methods

3.1. The formulation of the model

To investigate the effects of COVID-19 vaccination efforts and other epidemiological factors on the transmission of the virus in Nigerian, a non-linear mathematical model was designed. To better comprehend COVID-19 dynamics, the model was analyzed using deterministic mathematical analysis.

Utilizing S, S_V, E, I, H, D, and R,

$$N(t) = S(t) + S_V(t) + E(t) + I(t) + H(t) + D(t) + R(t). \quad (1)$$

The force of infection is a measure of the rate at which susceptible individuals become infected in a population, and it is computed by multiplying the population's infectious individuals by the chance of transmission from an infected individual to someone who is susceptible and by the rate of contact between the two people.

$$\frac{\beta(S + S_V)I}{N}. \quad (2)$$

A member of the susceptible population is someone who is at risk of contracting a disease. The recruitment of active individuals or new births causes the population of susceptible individuals to increase, while natural death causes the population to reduce. Therefore, the rate of change of the susceptible population is provided by

$$\frac{d^{\alpha} S(t)}{dt} = -\frac{\beta I(t) S(t)}{N} - \nu S + \psi S_v + \theta R. \quad (3)$$

The description of the interpersonal transmission coefficient as the rate of transmission per unit time per individual is given in the statement. It then explains how the population of vaccinated individuals changes over time, increasing with the rate of vaccination and decreasing with the rate of vaccination loss (deaths due to vaccination). The rate of change in the vaccinated population is then expressed mathematically.

$$\frac{d^{\alpha} S_V(t)}{dt} = -\frac{\beta I(t) S_V(t)}{N} + \nu S(t) - \psi S_v(t) - \rho S_V(t). \quad (4)$$

The statement explains the population of Exposed (E) individuals, which are infected but not yet infectious. Due to the force of infection, the population increases.$\frac{\beta(S(t)+S_V(t))I(t)}{N}$, which infects susceptible individuals, and decreases at rate σ as individuals

leave the exposed class. The rate of change of the exposed population is then expressed mathematically.

$$\frac{d^{\alpha}E(t)}{dt} = \frac{\beta}{N}(S + S_V I)(t) - \sigma E(t). \tag{5}$$

Individuals displaying COVID-19 symptoms are infectious, with their risk of contracting the virus increasing upon exposure .The rate of change of the infected population is then expressed mathematically.

$$\frac{d^{\alpha}I(t)}{dt} = \sigma E(t) - \gamma I(t). \tag{6}$$

The statement explains that the population of hospitalized individuals with COVID-19 symptoms increases from exposure to the virus via human-to-human transmission from symptomatic and super-spreader individuals. It further notes that this population decreases due to the natural death rate.

$$\frac{d^{\alpha}H(t)}{dt} = \phi\gamma(I(t) - \kappa H(t)). \tag{7}$$

The death compartment in COVID-19 modeling represents individuals who have died from the disease and is a vital part of understanding the pandemic's impact on public health. Accurately modeling the death compartment helps policymakers develop effective strategies for controlling the spread of the virus.

$$\frac{d^{\alpha}D(t)}{dt} = \varepsilon\phi\kappa H(t). \tag{8}$$

The statement explains that the population of recovered individuals consists of those who have recovered from COVID-19. This population increases at the recovery rate of non-hospitalized patients, while the recovery rate of hospitalized patients decreases.

$$\frac{d^{\alpha}R(t)}{dt} = (1-\phi)\gamma I(t) + (1-\varepsilon\phi)\kappa H(t) + \rho S_V(t) - \theta R(t). \tag{9}$$

The seven-compartment model of COVID-19 tracks the movement of individuals between compartments using differential equations that describe transmission, from susceptible to recovery. The model considers the impact of vaccination, with a compartment for vaccinated individuals that increases with recruitment and decreases with vaccination loss. The force of infection calculates the rate of transmission from infected to susceptible individuals.

$$\begin{aligned}
\frac{d^{\alpha}S(t)}{dt} &= -\frac{\beta}{N}S(t)I(t) + \psi S_V(t) - \nu S(t) + \theta R(t),\\
\frac{d^{\alpha}S_V(t)}{dt} &= -\frac{\beta}{N}S_V(t)I(t) - \psi S_V(t) + \nu S(t) - \rho S_V(t),\\
\frac{d^{\alpha}E(t)}{dt} &= \frac{\beta}{N}(S(t)I(t) + S_V(t)I(t)) - \sigma E(t),\\
\frac{d^{\alpha}I(t)}{dt} &= -\gamma I(t)\sigma E(t),\\
\frac{d^{\alpha}H(t)}{dt} &= \gamma\phi I(t) - \kappa H(t),\\
\frac{d^{\alpha}D(t)}{dt} &= \varepsilon\phi\kappa H(t),\\
\frac{d^{\alpha}R(t)}{dt} &= \gamma(1-\phi)I(t) + \rho S_V(t) + (1-\varepsilon\phi)\kappa H(t) - \theta R(t).
\end{aligned} \tag{10}$$

Table 1. Variables, parameters, descriptions and their values.

Variable	Description	Values	Refs
$S(t)$	Individual susceptible to the disease at time t	47000	[47]
$S_v(t)$	Vaccinated individual who are susceptible to the disease at time t	5000	[47]
$E(t)$	Infected individuals not yet infectious at time t	2003	[47]
$I(t)$	Individual who are currently infected and able to transmit at time	416	[47]
$H(t)$	Individuals who require hospitalization due to severe symptoms at time t	300	[47]
$D(t)$	Death individual at time t	150	[47]
$R(t)$	Individual at time t are those were previously infected	380	[47]
Parameter	**Description**	**Values**	**Refs**
β	Time-varying transmission rate	0.001	[47]
ν	Vaccination rate	0.125	[47]
ψ	Vaccine efficacy rate	0.05	[47]
κ	Rate of removal from the severity stage	0.001	[47]
ρ	Booster rate	0.9	[47]
σ	Rate of infectiousness onset after exposure	0.08	[47]
θ	Recovery rate	0.07	[47]
γ	Rate of loss of infectiousness	0.02	[47]
ϕ	Infection severity case ratio	0.02	[47]
ε	Severity case mortality ratio	0.027	[47]

The process of reformulating and analyzing the derivative in the Caputo fractional order mathematical model of the equation leads to model (11).

$$\begin{aligned}
{}^{C}J^{\alpha_1}S &= -\tfrac{\beta IS}{N} - \nu S(t) + \psi S_V + \theta R,\\
{}^{C}J^{\alpha_2}S_V &= -\tfrac{\beta IS_V}{N} + \nu S - \psi S_V - \rho S_V,\\
{}^{C}J^{\alpha_3}E &= \tfrac{\beta(S+S_V I}{N} - \sigma E,\\
{}^{C}J^{\alpha_4}I &= \sigma E - \gamma I,\\
{}^{C}J^{\alpha_5}H &= \phi\gamma(I - \kappa H),\\
{}^{C}J^{\alpha_6}D &= \varepsilon\phi\kappa H,\\
{}^{C}J^{\alpha_7}R &= (1-\phi)\gamma I + (1-\varepsilon\phi)\kappa H + \rho S_V - \theta R.
\end{aligned} \tag{11}$$

Table 1 presents the definition of each compartment and provides a description of each variable and parameter utilized in the model.

4. Model analysis

In this section, we will carry out a qualitative analysis of the mathematical model using an integer-order method. As a result, we will be able to thoroughly examine the attributes of the mathematical model and demonstrate how it may be put to use in actual scenarios.

4.1. Solution positivity and boundedness

The lemma that follows shows that the solutions to the equations in Model (11) are positive and bounded.

Lemma 1. Let $t_0 > 0$. If there are initial conditions in Model (11) such that $S(0) > 0$, $S_v(0) > 0$, $E(0) > 0$, $I(0) > 0$, $H(0) > 0$, $D(0) > 0$, and $R(0) > 0$, then for all $t \in [0, t_0]$, $S(t)$, $S_v(t)$, $E(t)$, $I(t)$, $H(t)$, $D(t)$, and $R(t)$ will remain bounded and positive in R_+^7.

Proof.

The model (11)'s first equation:

$$^{C}J^{\alpha_1}S(t) = -\frac{\beta}{N}S(t)I(t) + \psi S_v(t) - vS(t) + \psi R(t). \quad (12)$$

Solving for $S(t)$ yields:

$$S(t) > S(0)\ell^{-(v+\frac{\beta}{N})\int I(t)dt} > 0.$$

The second equation of the model (11)

$$^{C}J^{\alpha_2}S_v(t) = -\frac{\beta}{N}S_v(t)I(t) + vS(t) - \psi S_v(t) - bS_V(t). \quad (13)$$

Solving for $S_v(t)$ yields:

$$S_V(t) > S_V(0)\ell^{-(\psi+\frac{\beta}{N})\int I(t)dt} > 0.$$

The model (11)'s third equation:

$$^{C}J^{\alpha_3}E(t) = \frac{\beta}{N}(S(t)I(t) + S_v(t)I(t)) - \sigma E(t). \quad (14)$$

Solving for $E(t)$ yields:

$$E(t) > E(0)e^{-\sigma t} > 0.$$

The fourth equation of the model (11):

$$^{C}J^{\alpha_4}I(t) = -\gamma I(t) + \sigma E(t). \quad (15)$$

Solving for $I(t)$ yields:

$$I(t) > I(0)e^{-\gamma t} > 0.$$

The fifth equation of the model (11):

$$^{C}J^{\alpha_5}H(t) = -\gamma H(t) + \phi\gamma I(t). \quad (16)$$

Solving for $H(t)$ yields:

$$H(t) > H(0)e^{-\gamma t} > 0.$$

The sixth equation of the model (11):

$$^{C}J^{\alpha_6}D(t) = r\phi\kappa H(t). \quad (17)$$

Solving for $D(t)$ yields:

$$D(t) > D(0)e^{t} > 0.$$

The seventh equation of the model (11):

$$^{C}J^{\alpha_7}R(t) = \gamma(1-\phi)I(t)+\kappa(1-r\phi)H(t)+bS_v(t)-\psi R(t). \quad (18)$$

Solving for $R(t)$ yields:

$$R(t) > R(0)e^{-\psi t} > 0.$$

All these seven solutions have constants of integration given by $S(0)$ $S_V(0)$, $E(0)$, $I(0)$, $H(0)$, $D(0)$ and $R(0)$. Therefore for any time period $[0; t_0]$, $S(t), S_V(t), E(t), I(t), H(t), D(t)$ and $R(t)$ will be positive. It can be demonstrated that all seven equations will eventually be bounded for some value of t. As a result, Model (11) is both bounded above and bounded below. Since the model is positive and bounded, it is well-posed from both a mathematical and epidemiological perspective within the given region

4.2. Existence and uniqueness of model solution

In order to establish the existence and uniqueness of solutions for the fractional order system, we verify the Local Lipschitz condition, as provided by the preceding theorem.

Theorem 1: The system of equations satisfies the local Lipschitz condition if there is a constant Z for all t, t'in the neighborhood W of the initial conditions and for all $\omega \in (0, 1)$ such that:

$$\left| \begin{array}{l} J^{\alpha}\,[S(t),\, S_V(t),\, E(t), I(t), H(t), F(t), R(t)] \\ -J^{\alpha}\,[S(t'),\, S_V(t'),\, E(t'), I(t'), H(t'), F(t'), R(t')] \end{array} \right| \leq Z \left| \begin{array}{l} [S(t),\, S_V(t),\, E(t), I(t), H(t), F(t), R(t)] \\ -[S(t'),\, S_V(t'),\, E(t'), I(t'), H(t'), F(t'), R(t')] \end{array} \right|.$$

Proof: From equation (10), let:

$$\begin{aligned} g_1 &= -\tfrac{\beta I(t)S(t)}{N} - vS(t) + \psi S_v(t) + \theta R(t), \\ g_2 &= -\tfrac{\beta I(t)S_V(t)}{N} + vS(t) - \psi S_v(t) - \rho S_V(t), \\ g_3(S, S_V, E, I, H, F, R) &= \tfrac{\beta(S(t)+S_V(t))I(t)}{N} - \sigma E(t), \\ g_4 &= \sigma E(t) - \gamma I(t), \\ g_5 &= \phi\gamma(I(t) - \kappa H(t), \\ g_6 &= \varepsilon\phi\kappa H(t), \\ g_7 &= (1-\phi)\gamma I(t) + (1-\varepsilon\phi)\kappa H(t) + \rho S_V(t) - \theta R(t). \end{aligned}$$

Then the following inequality hold:

$$\left| \begin{array}{l} g(S, S_V, E, I, H, F, R) \\ - \\ g(S', S_V', E', I', H', F', R') \end{array} \right| \leq L \sqrt{\begin{array}{l} (S-S')^2 + \left(S_V - S_V'\right)^2 \\ +(E-E')^2 + (I-I')^2 \\ +(H-H')^2 + (F-F')^2 \\ +(R-R')^2. \end{array}},$$

where $N \geq \max(N1,\ N2, N3, N4, N5, N6, N7)$ and $N1,\ N2, N3, N4, N5, N6, N7$are the Lipchitz constants of each state variables.

Now, let:

$$N_1 = \max\left(\begin{array}{c} |\partial g_1/\partial S|,\ |\partial g_1/\partial S_V|,\ |\partial g_1/\partial E|,\ |\partial g_1/\partial I|, \\ |\partial g_1/\partial H|,\ |\partial g_1/\partial F|,\ |\partial g_1/\partial R| \end{array} \right),$$

$$N_2 = \max\left(\begin{array}{c} |\partial g_2/\partial S|,\ |\partial g_2/\partial S_V|,\ |\partial g_2/\partial E|,\ |\partial g_2/\partial I|, \\ |\partial g_2/\partial H|,\ |\partial g_2/\partial F|,\ |\partial g_2/\partial R| \end{array} \right),$$

$$N_3 = \max\left(\begin{array}{c} |\partial g_3/\partial S|,\ |\partial g_3/\partial S_V|,\ |\partial g_3/\partial E|,\ |\partial g_3/\partial I|, \\ |\partial g_3/\partial H|,\ |\partial g_3/\partial F|,\ |\partial g_3/\partial R| \end{array} \right),$$

$$N_4 = \max\left(\begin{array}{c} |\partial g_4/\partial S|,\ |\partial g_4/\partial S_V|,\ |\partial g_4/\partial E|,\ |\partial g_4/\partial I|, \\ |\partial g_4/\partial H|,\ |\partial g_4/\partial F|,\ |\partial g_4/\partial R| \end{array} \right),$$

$$N_5 = \max\begin{pmatrix} |\partial g_5/\partial S|, |\partial g_5/\partial S_V|, |\partial g_5/\partial E|, |\partial g_5/\partial I|, \\ |\partial g_5/\partial H|, |\partial g_5/\partial F|, |\partial g_5/\partial R| \end{pmatrix},$$

$$N_6 = \max\begin{pmatrix} |\partial g_6/\partial S|, |\partial g_6/\partial S_V|, |\partial g_6/\partial E|, |\partial g_6/\partial I|, \\ |\partial g_6/\partial H|, |\partial g_6/\partial F|, |\partial g_6/\partial R| \end{pmatrix},$$

$$N_7 = \max\begin{pmatrix} |\partial g_7/\partial S|, |\partial g_7/\partial S_V|, |\partial g_7/\partial E|, |\partial g_7/\partial I|, \\ |\partial g_7/\partial H|, |\partial g_7/\partial F|, |\partial g_7/\partial R| \end{pmatrix}.$$

Then,

$$N_1 = \max\left(\left|-v - \frac{\beta}{N}\right|, |\psi|, 0, \left|-\frac{\beta}{N}\right|, 0, 0, |\theta|\right),$$

$$N_2 = \max\left(\left|v - \frac{\beta}{N}\right|, |\psi + \rho|, 0, 0, 0, 0, 0\right),$$

$$N_3 = \max\left(\left|\frac{\beta I}{N}\right|, \left|\frac{\beta I}{N}\right|, |\sigma|, \left|\frac{\beta(S + S_V)}{N}\right|, 0, 0, 0, 0\right),$$

$$N_4 = \max(0, 0, |\sigma|, |\gamma|, 0, 0, 0),$$

$$N_5 = \max(0, 0, 0, |\phi\gamma|, |\kappa|, 0, 0),$$

$$N_6 = \max(0, 0, 0, 0, |\varepsilon\phi\kappa|, 0, 0),$$

$$N_7 = \max(0, |\rho|, 0, |(1-\phi)\gamma|, |(1-\varepsilon\phi)\kappa|, |\theta|).$$

Since the Lipchitz, condition is satisfied if there exist a constant $N \geq \max(N_1, N_2, N_3, N_4, N_5, N_6, N_7)$. Therefore, there is a unique solution for the system. Furthermore, since,$\max(N_1, N_2, N_3, N_4, N_5, N_6, N_7) \leq N \leq \infty$, this shows that the model's solution is bounded and exists for all time within the neighborhood of N.

Before arriving at an analytical answer, one must manipulate many mathematical concepts in order to find an exact, closed-form mathematical statement. In order to clearly explain the dynamics of the system, this approach seeks to express the solution in terms of well-known mathematical functions.

4.3. Disease free equilibrium point

The disease-free equilibrium point of the model is given as

$$E_0 = \left(\frac{\psi + \rho}{\upsilon}, 0, 0, 0, 0, 0, \frac{\rho}{\theta}\right).$$

4.4. Endemic equilibrium state

The endemic equilibrium, alternatively referred to as a non-zero equilibrium condition, arises when a disease continues to exist within a population. In contrast to the disease-free state $S_V = E = I = H = D = R \neq 0$. Thus, the endemic equilibrium state yields:

$$S^{**} = \frac{(\varepsilon\gamma\phi^2\psi + \varepsilon\gamma\phi^2\rho + \beta)N\gamma}{(\varepsilon\gamma\phi^2\psi + \varepsilon\gamma\phi^2\rho + \varepsilon\gamma\phi^2\upsilon + \beta)\beta},$$

$$S_V{}^{**} = \frac{\varepsilon\gamma\phi^2 N\gamma^2\upsilon}{(\varepsilon\gamma\phi^2\psi + \varepsilon\gamma\phi^2\rho + \varepsilon\gamma\phi^2\upsilon + \beta)\beta},$$

$$E^{**} = \frac{N}{\varepsilon\phi^2\sigma}, \qquad I^{**} = \frac{N}{\varepsilon\phi^2\gamma},$$

$$H^{**} = \frac{N}{\varepsilon\phi\kappa}, \qquad D^{**} = \frac{N}{\sigma\phi\gamma},$$

$$D^{**} = \frac{N}{\sigma\phi\gamma},$$

$$R^* \frac{N(\varepsilon^2\gamma^2\phi^4\rho\upsilon - \beta\varepsilon^2\gamma\phi^4\psi - \beta\varepsilon^2\gamma\phi^4\rho - \beta\varepsilon^2\gamma\phi^4\upsilon + \beta\varepsilon\gamma\phi^2\psi + \beta\varepsilon^2\gamma\phi^4\rho + \beta\varepsilon^2\gamma\phi^4\upsilon - \beta^2\varepsilon\phi^2 + \beta^2)}{\theta(\varepsilon\gamma\phi^2\psi + \varepsilon\gamma\phi^2\rho + \varepsilon\gamma\phi^2\upsilon + \beta)\beta\varepsilon\phi^2}.$$

4.5. Basic reproduction number

The basic reproduction ration of the system is obtained as

$$R_0 = \frac{\beta(\psi + \rho)}{\gamma\upsilon}.$$

5. Model solution via Laplace-Adomian Decomposition Method application (LADM)

In this section, the LADM shall be applied to obtain the approximate solution for the mathematical model (11) analytically. This is initiated by taking the Laplace transforms of both sides of model (11) to obtain

$$\begin{aligned}
L\{{}^C J^{\alpha_1} S(t)\} &= L\{-\frac{\beta I(t)S(t)}{N} - vS(t) + \psi S_v(t) + \psi R(t)\},\\
L\{{}^C J^{\alpha_2} S_V(t)\} &= -L\{\frac{\beta I(t)S_V(t)}{N} + vS(t) - \psi S_v(t) - bS_V(t)\},\\
L\{{}^C J^{\alpha_3} E(t)\} &= L\{\frac{\beta(S(t) + S_V(t))I(t)}{N} - \sigma E(t)\},\\
L\{{}^C J^{\alpha_4} I(t)\} &= L\{\sigma E(t) - \gamma I(t)\},\\
L\{{}^C J^{\alpha_5} H(t)\} &= L\{\phi\gamma(I(t) - \gamma H(t))\},\\
L\{{}^C J^{\alpha_6} D(t)\} &= L\{r\phi\kappa H(t)\},\\
L\{{}^C J^{\alpha_7} R(t)\} &= L\{(1-\phi)\gamma I(t) + (1 - r\phi)\kappa H(t) + bS_V(t) - \psi R(t)\}.
\end{aligned}$$

Applying Definition 4 to the preceding equation and then simplifying, we obtain

$$\begin{aligned}
S &= S^{-1}S(0) + \frac{1}{S^{\alpha_1}}L\left\{-\frac{\beta IS}{N} - vS + \psi S_v + \psi R\right\},\\
S_V &= S^{-1}S_V(0) + \frac{1}{S^{\alpha_2}}L\left\{-\frac{\beta IS_V}{N} + vS - \psi S_v - bS_V\right\},\\
E &= S^{-1}E(0) + \frac{1}{S^{\alpha_3}}L\left\{\frac{\beta(S + S_V)I}{N} - \sigma E\right\},\\
I &= S^{-1}I(0) + \frac{1}{S^{\alpha_4}}L\{\sigma E - \gamma I\},\\
H &= S^{-1}H(0) + \frac{1}{S^{\alpha_5}}L\{\phi\gamma(I - \gamma H)\},\\
D &= S^{-1}D(0) + \frac{1}{S^{\alpha_6}}L\{r\phi\kappa H\},\\
R &= S^{-1}R(0) + \frac{1}{S^{\alpha_7}}L\{(1-\phi)\gamma I + (1 - r\phi)\kappa H + bS_V - \psi R\}.
\end{aligned} \tag{19}$$

Representing the solutions $S(t)$, $S_V(t)$, $E(t)$, $I(t)$, $H(t)$, $D(t)$ and $R(t)$ in the form of infinite series:

$$\begin{aligned} S(t) &= \sum_{n=0}^{\infty} S_n, \quad S_V(t) = \sum_{n=0}^{\infty} S_{V_n}, \\ E(t) &= \sum_{n=0}^{\infty} E_n, \quad I(t) = \sum_{n=0}^{\infty} I_n, \\ H(t) &= \sum_{n=0}^{\infty} H_n, \quad D(t) = \sum_{n=0}^{\infty} D_n, \\ R(t) &= \sum_{n=0}^{\infty} R_n. \end{aligned} \tag{20}$$

The nonlinear terms of the model $S(t)I(t), S_V(t)I(t)$ can be decomposed by Adomain polynomials given by Definition 5:

$$S(t)I(t) = \sum_{n=0}^{\infty} A_n, \quad S_V(t)I(t) = \sum_{n=0}^{\infty} B_n, \tag{21}$$

where A_n, B_n are Adomain polynomials given by

$$A_n = \frac{1}{\Gamma(n+1)} \frac{d^n}{dt} \left[\sum_{k=0}^{n} \lambda^k I_k \sum_{k=0}^{n} \lambda^n S_k \right] \lambda, \tag{22}$$

$$B_n = \frac{1}{\Gamma(n+1)} \frac{d^n}{dt} \left[\sum_{k=0}^{n} \lambda^k S_{V_k} \sum_{k=0}^{n} \lambda^n I_k \right] \lambda. \tag{23}$$

Evaluating equation (19) using equations (20) and (21) yields

$$\begin{aligned} S &= S^{-1}S(0) + \tfrac{1}{S^{\alpha_1}} L\{-KA_n - \nu S_n + \psi S_{Vn} + \theta R_n\}, \\ S_V &= S^{-1}V(0) + \tfrac{1}{S^{\alpha_2}} L\{-KB_n + \nu S_n - \psi S_{Vn} - bS_{Vn}\}, \\ E &= S^{-1}E(0) + \tfrac{1}{S^{\alpha_3}} L\{K(A_n + B_n) - \sigma E_n\}, \\ I &= S^{-1}I(0) + \tfrac{1}{S^{\alpha_4}} L\{\sigma E_n - \gamma I_n\}, \\ H &= S^{-1}P(0) + \tfrac{1}{S^{\alpha_5}} L\{\phi\gamma I_n - \kappa H_n\}, \\ D &= S^{-1}A(0) + \tfrac{1}{S^{\alpha_6}} L\{r\phi\kappa H_n\}, \\ R &= S^{-1}H(0) + \tfrac{1}{S^{\alpha_7}} L\{(1-\phi)\gamma I_n, \\ &+(1-r\phi)\kappa H_n - bS_V - \theta R_n\}. \end{aligned} \tag{24}$$

Using initial conditions in equation (24), we have:

$$\begin{aligned} S(t) &= \frac{n_1}{S} + \frac{1}{S^{\alpha_1}} L\{-KA_n - \nu S_n + \psi S_{Vn} + \theta R_n\}, \\ S_V(t) &= \frac{n_2}{S} + \frac{1}{S^{\alpha_2}} L\{-KB_n + \nu S_n - \psi S_{Vn} - bS_{Vn}\}, \\ E(t) &= \frac{n_3}{S} + \frac{1}{S^{\alpha_3}} L\{K(A_n + B_n) - \sigma E_n\}, \\ I(t) &= \frac{n_4}{S} + \frac{1}{S^{\alpha_4}} L\{\sigma E_n - \gamma I_n\}, \\ H(t) &= \frac{n_5}{S} + \frac{1}{S^{\alpha_5}} L\{\phi\gamma I_n - \kappa H_n\}, \\ D(t) &= \frac{n_6}{S} + \frac{1}{S^{\alpha_6}} L\{r\phi\kappa H_n\}, \\ R(t) &= \frac{n_7}{S} + \frac{1}{S^{\alpha_7}} L\{(1-\phi)\gamma I_n + (1-r\phi)\kappa H_n - bS_V - \theta R_n\}. \end{aligned} \tag{25}$$

To get the solution of each compartment, we iterate the terms in equation (25) and take the Laplace inverse to give the general formula for the model:

$$\begin{aligned} &\textstyle\sum_{n=0}^{\infty} S_{n+1} = \mathcal{L}^{-1}\left[\frac{1}{S^{\alpha_1}}\mathcal{L}\{-KA_n - \nu S_n + \psi S_{Vn} + \theta R_n\}\right], \\ &\textstyle\sum_{n=0}^{\infty} S_{Vn+1} = \mathcal{L}^{-1}\left[\frac{1}{S^{\alpha_2}}\mathcal{L}\{-KB_n + \nu S_n - \psi S_{Vn} - bS_{Vn}\}\right], \\ &\textstyle\sum_{n=0}^{\infty} E_{n+1} = \mathcal{L}^{-1}\left[\frac{1}{S^{\alpha_3}}\mathcal{L}\{K(A_n + B_n) - \sigma E_n\}\right], \\ &\textstyle\sum_{n=0}^{\infty} I_{n+1} = \mathcal{L}^{-1}\left[\frac{1}{S^{\alpha_4}}\mathcal{L}\{\sigma E_n - \gamma I_n\}\right], \\ &\textstyle\sum_{n=0}^{\infty} H_{n+1} = \mathcal{L}^{-1}\left[\frac{1}{S^{\alpha_5}}\mathcal{L}\{\phi\gamma I_n - \kappa H_n\}\right], \\ &\textstyle\sum_{n=0}^{\infty} D_{n+1} = \mathcal{L}^{-1}\left[\frac{1}{S^{\alpha_6}}\mathcal{L}\{r\phi\kappa H_n\}\right], \\ &\textstyle\sum_{n=0}^{\infty} R_{n+1} = \mathcal{L}^{-1}\left[\frac{1}{S^{\alpha_8}}\mathcal{L}\{(1-\phi)\gamma I_n\right], \\ &+\left[(1-r\phi)\kappa H_n - bS_V - \theta R_n\right]. \end{aligned} \tag{26}$$

The following values were obtained from system (26):

$$\begin{aligned} &S_0 = n_1, \quad S_{V0} = n_2, \quad E_0 = n_3, \quad I_0 = n_4, \\ &H_0 = n_5, \quad D_0 = n_6, \quad R_0 = n_7. \end{aligned} \tag{27}$$

$$\begin{aligned} S_1 &= (-Kn_4n_1 - \nu n_1 + \psi n_2 + \theta n_7)\frac{t^{\alpha_1}}{\Gamma(\alpha_1+1)}, \\ S_{V_1} &= (-Kn_2n_4 + \nu n_1 - \psi n_2 - bn_2)\frac{t^{\alpha_2}}{\Gamma(\alpha_2+1)}, \\ E_1 &= (K(n_4n_1 + n_4n_2) - \sigma n_2)\frac{t^{\alpha_3}}{\Gamma(\alpha_3+1)}, \\ I_1 &= (\sigma n_2 - \gamma n_4)\frac{t^{\alpha_4}}{\Gamma(\alpha_4+1)}, \\ H_1 &= (\phi\gamma n_4 - \kappa n_5)\frac{t^{\alpha_5}}{\Gamma(\alpha_5+1)}, \\ D_1 &= (r\phi\kappa n_5)\frac{t^{\alpha_6}}{\Gamma(\alpha_6+1)}, \\ R_1 &= ((1-\phi)\gamma n_4 + (1-r\phi)\kappa n_5 - bn_2 - \theta n_7)\frac{t^{\alpha_7}}{\Gamma(\alpha_7+1)}. \end{aligned}$$

Evaluating the results obtained with the baseline parameter values provided in Table 1, we derive the following series

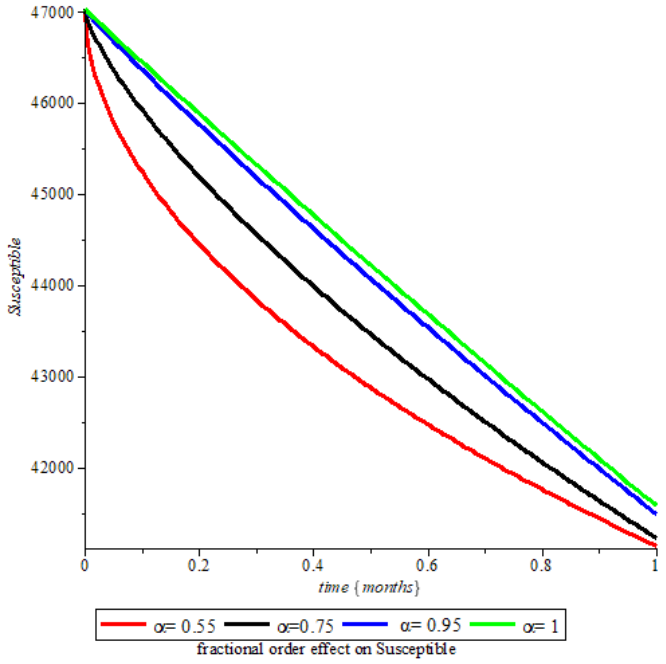

Figure 1. Effect of fractional order α on $S(t)$.

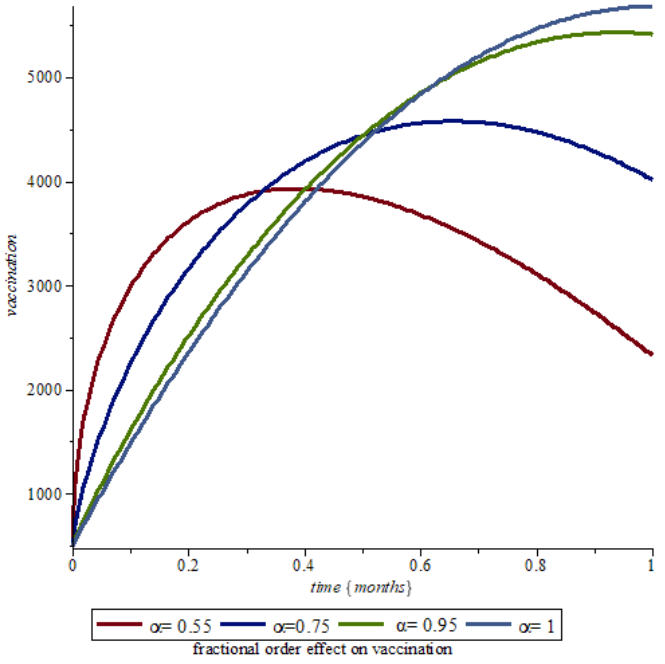

Figure 2. Effect of fractional order α on $V(t)$.

solution of arbitrary order:

$$
\begin{aligned}
S &= 47000 - \frac{5750.919622t^{\alpha}}{\Gamma(\alpha+1)} + \frac{622.4360875t^{2\alpha}}{\Gamma(2\alpha+1)},\\
S_V &= 500 + \frac{10277.49791t^{\alpha}}{\Gamma(\alpha+1)} - \frac{10189.05057t^{2\alpha}}{\Gamma(2\alpha+1)},\\
E &= 2003 - \frac{400.021787t^{\alpha}}{\Gamma(\alpha+1)} - \frac{31.99000457t^{2\alpha}}{\Gamma(2\alpha+1)},\\
I &= 416 + \frac{316.80t^{\alpha}}{\Gamma(\alpha+1)} + \frac{758.8398328t^{2\alpha}}{\Gamma(2\alpha+1)},\\
H &= 300 + \frac{41.300t^{\alpha}}{\Gamma(\alpha+1)} + \frac{31.638700t^{2\alpha}}{\Gamma(2\alpha+1)},\\
D &= 150 + \frac{0.400500t^{\alpha}}{\Gamma(\alpha+1)} + \frac{0.00055135500t^{2\alpha}}{\Gamma(2\alpha+1)},\\
R &= 380 - \frac{4484.70400t^{\alpha}}{\Gamma(\alpha+1)} - \frac{8904.098090t^{2\alpha}}{\Gamma(2\alpha+1)}.
\end{aligned}
\tag{28}
$$

5.1. Numerical simulations

Experiment I: Fractional order analysis of the model transmission dynamics

The fractional order analysis of the COVID-19 model, depicted in Figures 1 to 7, provides crucial insights. These figures illustrate integral curves of state variables across a range of alpha values (0.55–1), unveiling distinct patterns.

In Figure 1, a notable declination of susceptibility is observed as alpha increases (0.55–1), this is attributed to a more effective vaccination and enhanced disease control measures. Figure 2 sheds light on the dynamics of vaccination growth. Vaccination growth is slower at integer orders and accelerates at fractional orders, emphasizing the critical role of precise timing and comprehensive vaccine coverage in pandemic

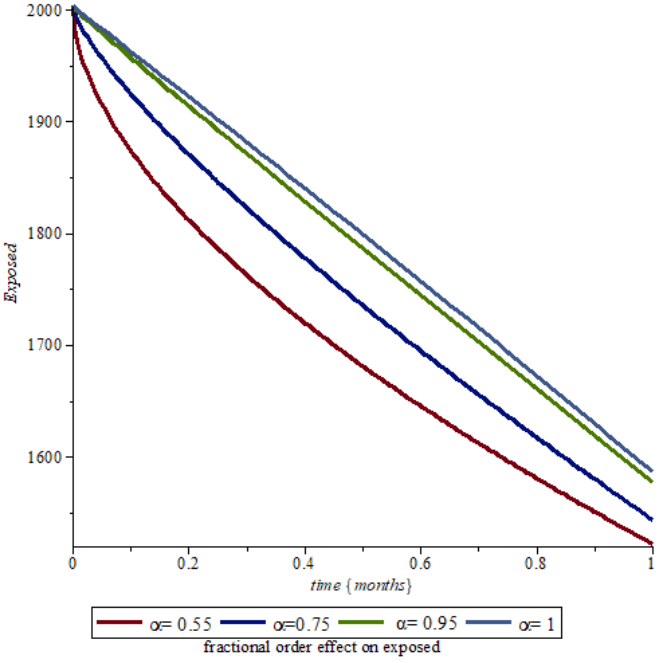

Figure 3. Effect of fractional order α on $E(t)$.

management. Figures 3, 4 and 5 draw attention to the exposure–infection–hospital conversion rate. This process occurs more rapidly at higher α values and more slowly at lower fractional orders, highlighting the significance of alpha in pandemic progression. In Figure 6, a reduction in the death rate at the integer level is evident, showcasing the positive influence of vaccination on lowering mortality. Simultaneously, Figure 7 illustrates a substantial rise in the recovery level of individuals as

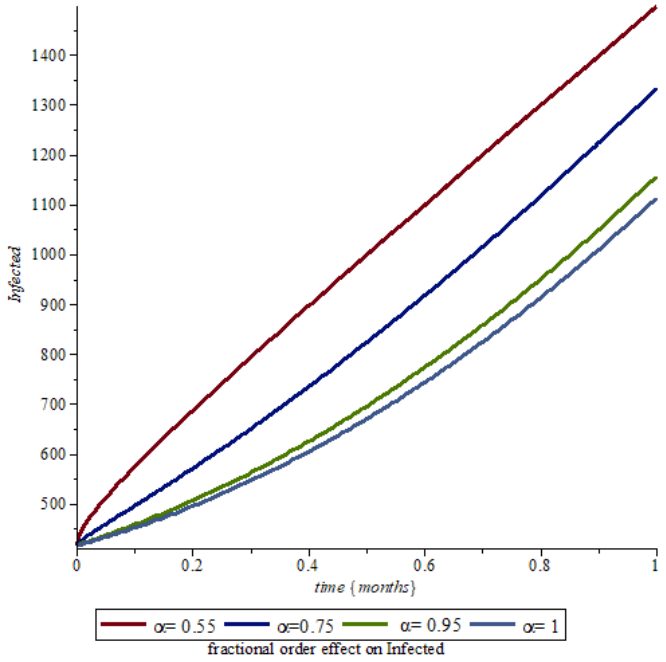

Figure 4. Effect of fractional order α on $I(t)$.

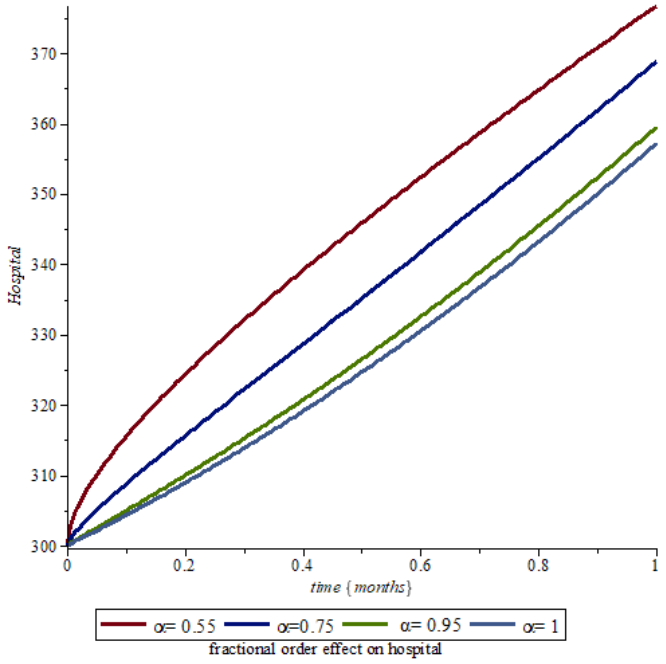

Figure 5. Effect of fractional order α on $H(t)$.

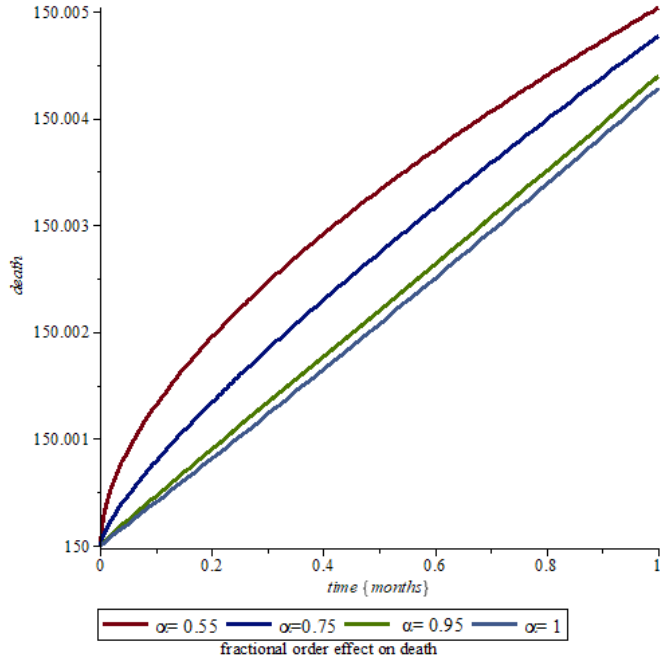

Figure 6. Effect of fractional order α on $D(t)$.

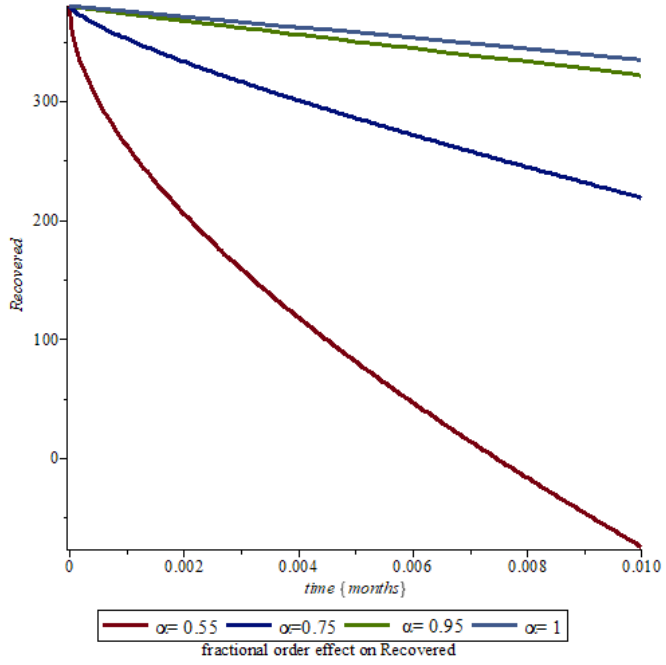

Figure 7. Effect of fractional order α on $R(t)$.

the fractional order increases.

Experiment II: Assessment of Transmission Rate in Susceptible, Vaccinated, and Exposed Populations

The simulation results depicted in Figures 8, 9, 10, 11, 12 and 13 explore the influence of the transmission rate on susceptible, vaccinated, and exposed populations under both integer and fractional-order scenarios. We analyze how this parameter affects disease spread in classical and fractional-order models. The results reveal an increase in the recovery rate of individuals with the growth of α, while human susceptibility tends to decrease in fractional-order scenarios. Furthermore, the observed trends show a rapid decrease in the exposed population in classical order, whereas the vaccinated population is lower in fractional-order transmission rates.

Experiment III: Assessment of the Rate of Vaccine in a Susceptible Vaccinated Population

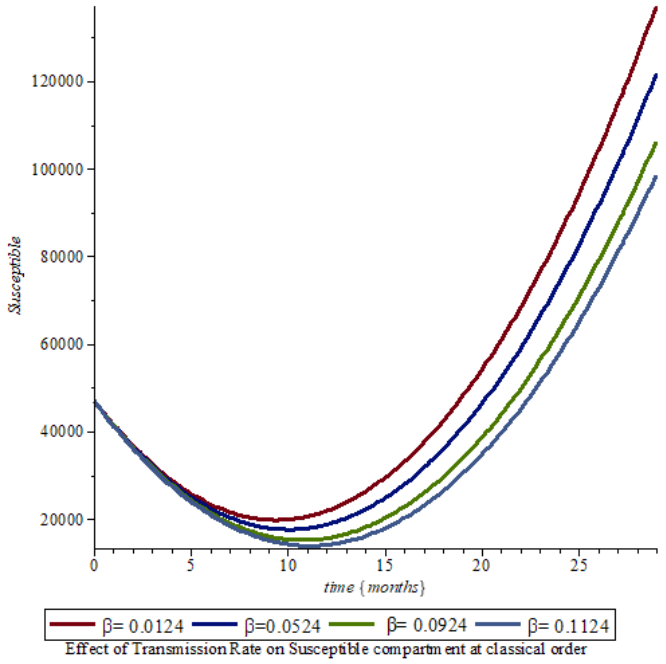

Figure 8. Effect of Transmission Rate β on $S(t)$. Classical sense.

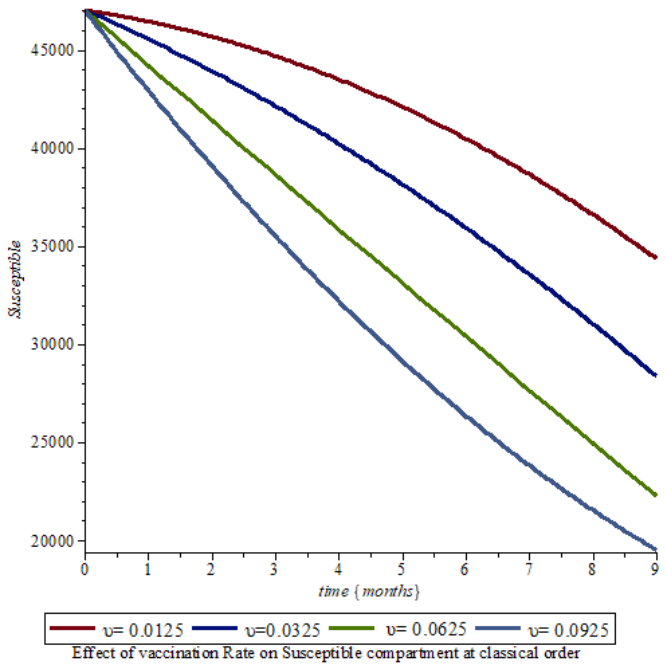

Figure 9. Effect of Transmission Rate β on $S(t)$. Fractional sense.

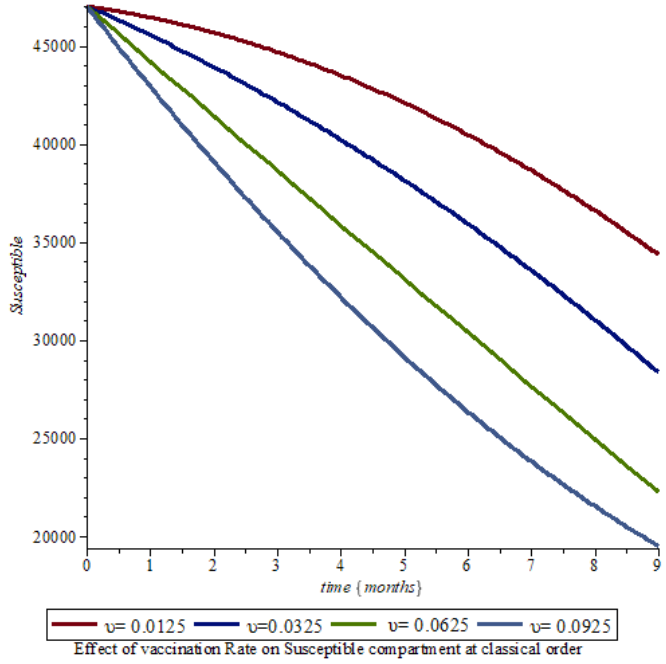

Figure 10. Effect of Transmission Rate β on $V(t)$. Classical sense.

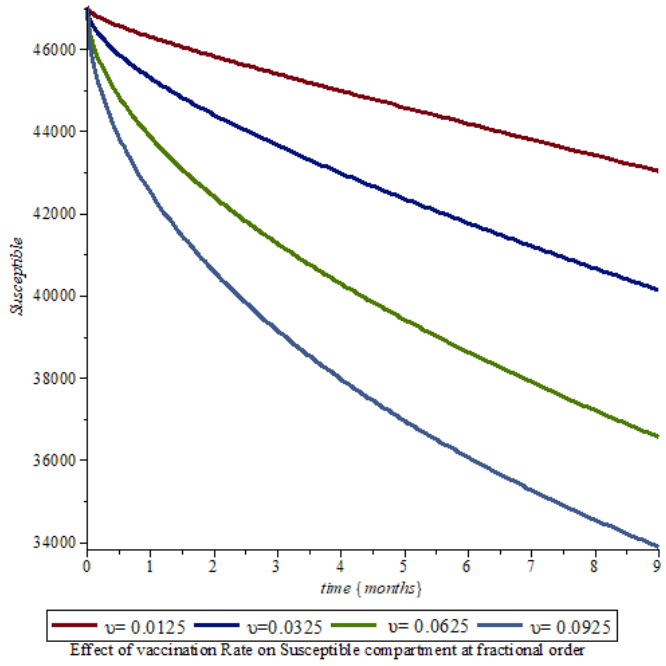

Figure 11. Effect of transmission rate β on $V(t)$ fractional sense.

We investigate the decline in immunity post-initial vaccine doses and the dynamics of first-dose vaccination in our effort to reduce new COVID-19 cases. Numerical experiments using our model offer insights into how these factors influence disease prevalence. The analysis is complemented by Figures 14, 15, 16, and 17, which highlight the vaccine administration rate and the impact of classical and fractional-order frameworks on individuals. This assessment enhances our understanding of vaccination dynamics underscoring that higher fractional order value of α and increased vaccination rates will lead to enhanced disease control.

6. Discussion of results and conclusion

6.1. Discussion of results

The study uses numerical simulations with the Caputo-derivative operator in a COVID-19 model with fractional orders

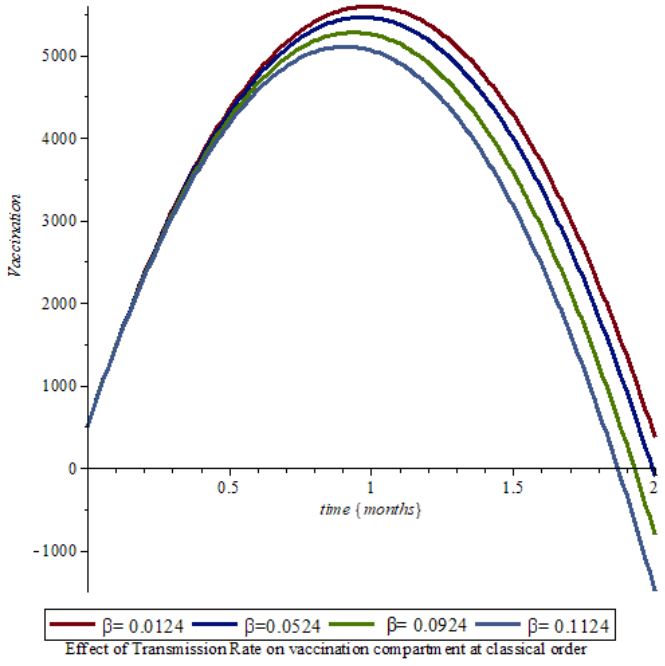

Figure 12. Effect of Transmission Rate β on $E(t)$. Classical sense.

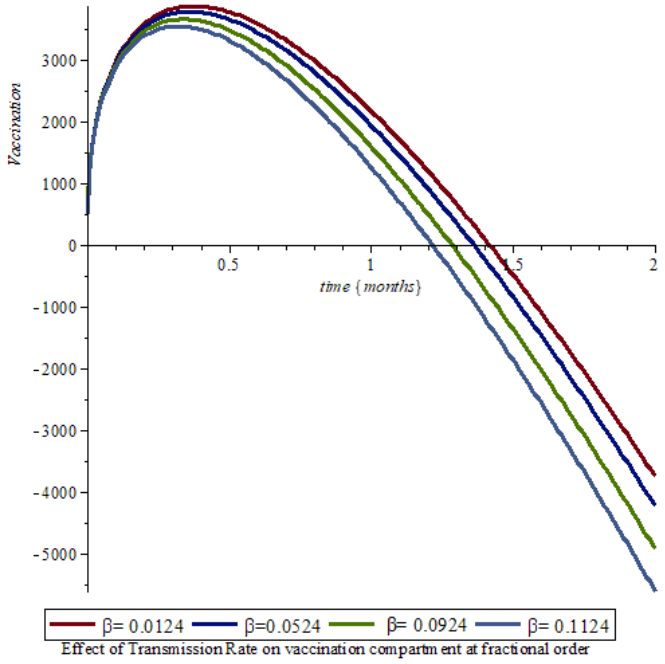

Figure 13. Effect of Transmission Rate β on $E(t)$. fractional sense

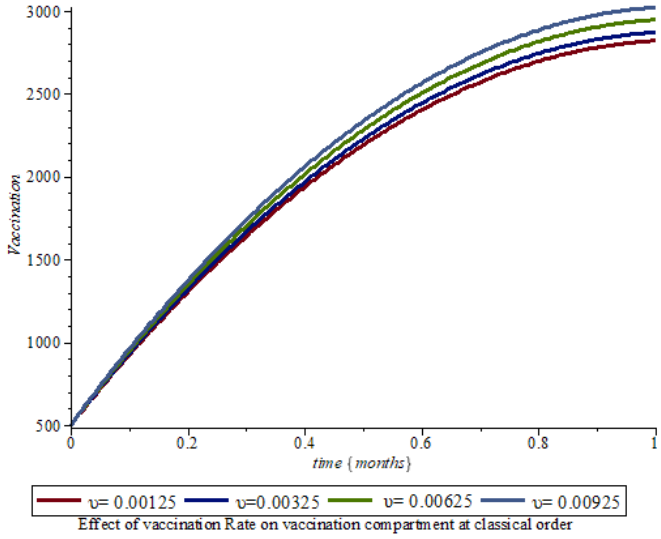

Figure 14. Effect of Vaccination Rate υ on $S(t)$. Classical sense.

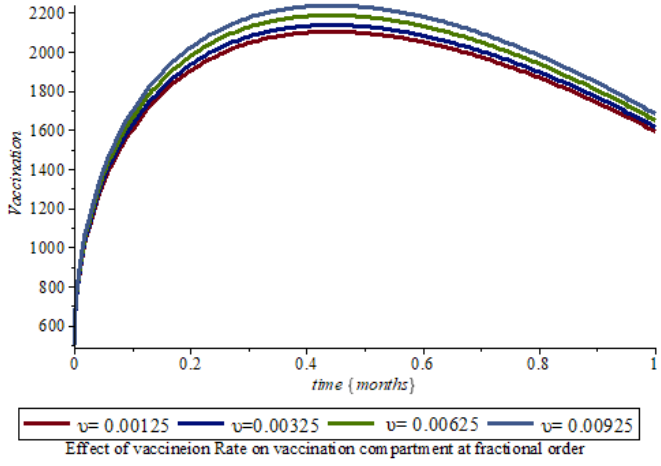

Figure 15. Effect of Vaccination Rate υ on $S(t)$. Fractional sense.

to model vaccination campaign effectiveness. The simulations use the Laplace-Adomian decomposition method. The research validates the Caputo fractional order derivative's effectiveness through convergence analysis. The fractional order COVID-19 model, depicted in Figures 1 through 7, shows enhanced adaptability, enabling outcome customization within model compartments.

The manuscript additionally underscores an intriguing observation pertaining to the anticipation of exceedingly low initial values. It underscores the considerable attention garnered by the impact of vaccination on COVID-19. Empirical evidence demonstrates that higher vaccination rates correlate with reduced mortality rates, as evidenced by the graphical representations in Figures 8 through 17. Vaccines function by bolstering an individual's immune system, rendering them less susceptible to the virus, and mitigating symptom severity. Widespread vaccination curtails virus transmission, leading to diminished incidence and fatalities. Furthermore, vaccination initiatives contribute to the establishment of herd immunity, a pivotal factor in curtailing community-wide virus transmission. Using Maple 18's Runge-Kutta order four (RK-4) solution, Figure 18 illustrates a comparison between the LADM ($\alpha = 1$) and RK-4 solutions for the susceptible class. The significant level of correlation emphasizes the effectiveness of LADM in solving the mathematical model.

The transmission rate emerges as a pivotal determinant

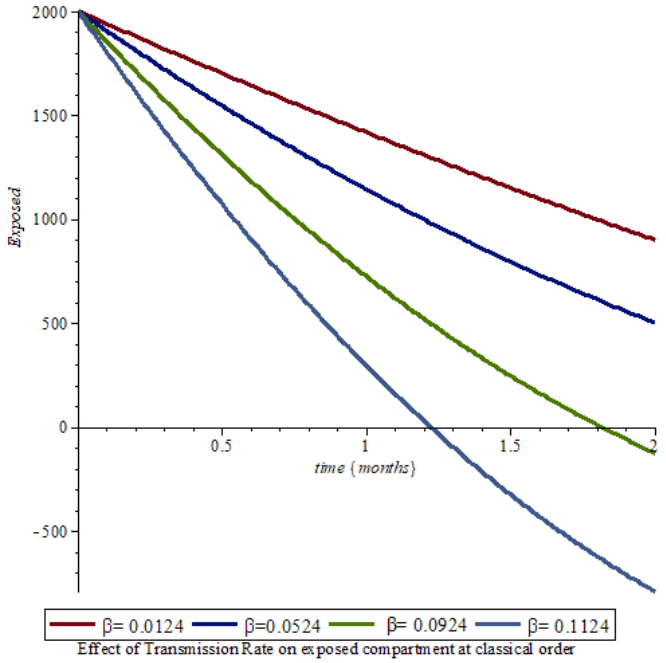

Figure 16. Effect of vaccination Rate υ on $V(t)$ classical sense.

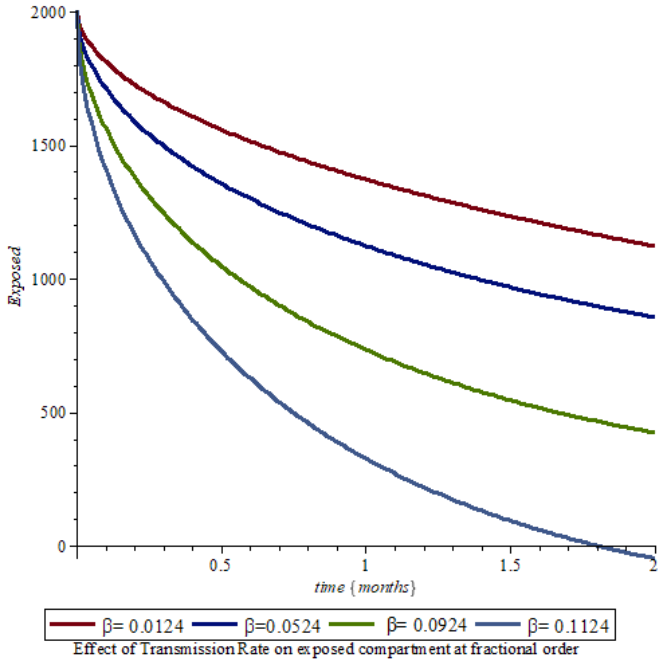

Figure 17. Effect of vaccination Rate υ on $V(t)$ fractional sense.

of the COVID-19 model's mortality rate. Lowering this rate through measures such as social distancing, mask-wearing, and improved ventilation is pivotal in reducing the number of cases and fatalities. In conclusion, vaccination exerts a pivotal influence on diminishing COVID-19-related fatalities. However, manipulating the fractional order value yields superior outcomes, notably decreasing the mortality rate with a lower transmission rate. Varying fractional order α in the model used in

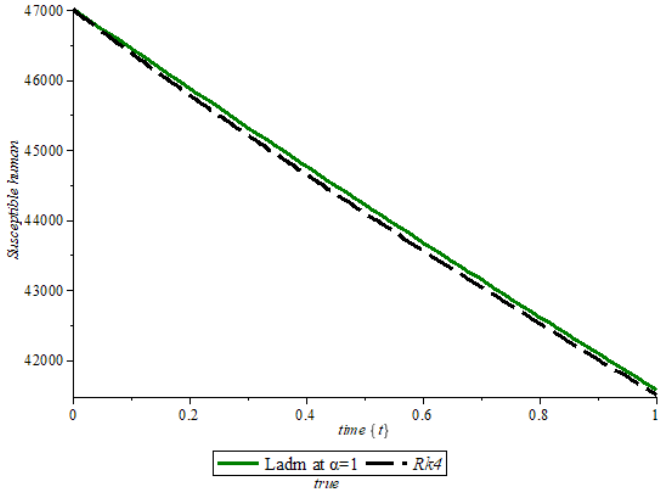

Figure 18. Comparison graph of standard numerical scheme $RK-4$ and LADM at fractional order $\alpha = 1$.

this study captures complex dynamics and non-linear interactions, allowing for the modeling of heterogeneous transmission patterns, memory effects, and intricate host-pathogen dynamics. Despite challenges in parameter estimation, it shows promise in understanding disease spread and optimizing interventions, and it aims to enhance the realistic depiction of epidemiological systems.

In summary, our findings indicate that employing fractional order modeling associated with vaccination campaign is linked to a general pattern of heightened susceptibility, increased rates of recovery, and a decrease in the overall number of infected individuals.

6.2. Conclusion

The convergent solution for mathematical models based on systems of differential equations may be computed more quickly using the Laplace-Adomian decomposition method, and this is a crucial point to remember. The unconditionally convergent Laplace-Adomian Decomposition Method (LADM) scheme for evaluating the vaccine impact on coronavirus disease is dynamically consistent, easy to implement, and exhibits good agreement to analyze the impact of corona viruses for a long period of time and depicts their dynamical behavior graphically. The positivity and boundedness of the solutions, as well as the usage of LADM to arrive at the analytical solution, were all used to quantify the model's validity. After the model's assumption regarding the rate of vaccination was taken into account, these calculations were further supported. Numerical simulations are run in order to confirm the model's real-world behavior.

Acknowledgment

The authors extend their heartfelt gratitude to all individuals who have contributed to the success of this research endeavor.

References

[1] M. Amin, M. Farman, A. Akgul & R. T. Alqahtani, "Effect of vaccination to control COVID-19 with fractal fractional operator", Alexandria Engineering Journal **61** (2022) 3551. https://doi.org/10.1016/j.aej.2021.09.006.

[2] T. Hussain, M. Ozair, F. Ali, S. urRehman, T. A. Assiri & E. E. Mahmoud,"Sensitivity analysis and optimal control of COVID-19 dynamics based on SEIQR model", Results in Physics **22** (2021) 103956. https://doi.org/10.1016/j.rinp.2021.103956.

[3] S. Khajanchi, K. Sarkar, J. Mondal, K. S. Nisar & S. F. Abdelwahab, "Mathematical modeling of the COVID-19 pandemic with intervention strategies", Results in Physics **25** (2021) 104285. https://doi.org/10.1016/j.rinp.2021.104285.

[4] M. K. Kolawole, M. O. Olayiwola, A. I. Alaje, H. O. Adekunle & K. A. Odeyemi, "Conceptual analysis of the combined effects of vaccination, therapeutic actions, and human subjection to physical constraint in reducing the prevalence of COVID-19 using the homotopy perturbation method", Beni-Suef University Journal of Basic and Applied Sciences **12** (2023) 1. https://doi.org/10.1186/s43088-023-00343-2.

[5] K. Abbas, S. R. Procter, K. Van Zandvoort, A. Clark, S. Funk, T. Mengistu & G. Medley, "Routine childhood immunisation during the COVID-19 pandemic in Africa: a benefit-risk analysis of health benefits versus excess risk of SARS-CoV-2 infection", The Lancet Global Health **8** (2020) 1264. https://doi.org/10.1016/S2214-109X(20)30308-9.

[6] A. Muniyappan, B. Sundarappan, P. Manoharan, M. Hamdi, K. Raahemifar, S. Bourouis & V. Varadarajan, "Stability and numerical solutions of second wave mathematical modeling on COVID-19 and Omicron outbreak strategy of pandemic: Analytical and error analysis of approximate series solutions by using HPM", Mathematics **10** (2022) 343. https://doi.org/10.3390/math10030343.

[7] A. I. Alaje, M. O. Olayiwola, K. A. Adedokun, J. A. Adedeji & A. O. Oladapo, "Modified homotopy perturbation method and its application to analytical solitons of fractional-order Korteweg–de Vries equation", Beni-Suef University Journal of Basic and Applied Sciences **11** (2022) 139. https://doi.org/10.1186/s43088-022-00317-w.

[8] B. G. Masresha, R. Luce Jr, M. E. Shibeshi, B. Ntsama, A. N'Diaye, J. Chakauya & R. Mihigo, "The performance of routine immunization in selected African countries during the first six months of the COVID-19 pandemic", The Pan African Medical Journal **37** (2020) https://doi.org/10.11604/pamj.supp.2020.37.1.26107.

[9] K. A. Gaythorpe, K. Abbas, J. Huber, A. Karachaliou, N. Thakkar, K. Woodruff and M. Jit, "Impact of COVID-19-related disruptions to measles, meningococcal A and yellow fever vaccination in 10 countries", Elife **10** (2021) 67023. https://doi.org/10.1016/j.vaccine.2022.05.074.

[10] M. Coker, M. O. Folayan, I. C. Michelow, R. E. Oladokun, N. Torbunde & N. A. Sam-Agudu, "Things must not fall apart: the ripple effects of the COVID-19 pandemic on children in sub-Saharan Africa", Pediatric Research **89** (2021) 1078. https://doi.org/10.1038/s41390-020-01174-y.

[11] A. Shet, K. Carr, M. C. Danovaro-Holliday, S. V. Sodha, C. Prosperi, J. Wunderlich & A. Lindstrand, "Impact of the SARS-CoV-2 pandemic on routine immunization services: evidence of disruption and recovery from 170 countries and territories", The Lancet Global Health **10** (2022) 186. https://doi.org/10.1016/S2214-109X(21)00512-X.

[12] E. Leshem & A. Wilder-Smith "COVID-19 vaccine impact in Israel and a way out of the pandemic", The Lancet **397** (2021) 1783. https://doi.org/10.1016/S2214-109X(21)00512-X.

[13] J. P. Figueroa, M. E. Bottazzi, P. Hotez, C. Batista, O. Ergonul, S. Gilbert & G. Kang, "Urgent needs of low-income and middle-income countries for COVID-19 vaccines and therapeutics", The Lancet **397** (2021) 562. https://doi.org/10.17615/htxb-an45.

[14] B. Chen, Y. Zhao, Z. Jin, D. He & H. Li, "Twice evasions of Omicron variants explain the temporal patterns in six Asian and Oceanic countries", BMC Infectious Diseases **23** (2023) 1. https://doi.org/10.1186/s12879-023-07984-9.

[15] S. K. Yadav, V. Kumar & Y. Akhter, "Modeling global COVID-19 dissemination data after the emergence of Omicron variant using multipronged approaches", Current Microbiology **79** (2022) 286. https://doi.org/10.3389/fpubh.2021.783201.

[16] O. M. Otunuga, "Analysis of multi-strain infection of vaccinated and recovered population through epidemic model: Application to COVID-19", Plos one **17** (2022) e0271446. https://doi.org/10.1371/journal.pone.0271446.

[17] M. Lounis, D. Bencherit, M. A. Rais & A. Riad, "COVID-19 vaccine booster hesitancy (VBH) and its drivers in Algeria: national cross-sectional survey-based study", Vaccines **10** (2022) 621. https://doi.org/10.3390/vaccines10040621.

[18] A. O. Yunus, M. O. Olayiwola, K. A. Adedokun, J. A. Adedeji & A. I. Alaje, "Mathematical analysis of fractional-order Caputo's derivative of coronavirus disease model via Laplace Adomian decomposition method", Beni-Suef University Journal of Basic and Applied Sciences **11** (2022) 144. https://doi.org/10.1186/s43088-022-00326-9.

[19] A. Boudaoui, Y. E hadjMoussa, Z. Hammouch & S. Ullah, "A fractional-order model describing the dynamics of the novel coronavirus (COVID-19) with nonsingular kernel", Chaos, Solitons & Fractals **146** (2021) 110859. https://doi.org/10.1016/j.chaos.2021.110859.

[20] A. Babaei, M. Ahmadi, H. Jafari & A. Liya, "A mathematical model to examine the effect of quarantine on the spread of coronavirus", Chaos, Solitons & Fractals **142** (2021) 110418. https://doi.org/10.1016/j.chaos.2020.110418.

[21] M. Arfan, M. M. Lashin, P. Sunthrayuth, K. Shah, A. Ullah, K. Iskakova & T. Abdeljawad, "On nonlinear dynamics of COVID-19 disease model corresponding to nonsingular fractional order derivative", Medical & Biological Engineering & Computing **60** (2022) 3169. https://doi.org/10.1007/s11517-022-02661-6.

[22] N. Debbouche, A. Ouannas, I. M. Batiha & G. Grassi, "Chaotic dynamics in a novel COVID-19 pandemic model described by commensurate and incommensurate fractional-order derivatives", Nonlinear Dynamics **2021** (2021) 1. https://doi.org/10.1007/s11071-021-06867-5.

[23] A. Ali, M. Y. Khan, M. Sinan, F. M. Allehiany, E. E. Mahmoud, A. H. Abdel-Aty & G. Ali, "Theoretical and numerical analysis of novel COVID-19 via fractional order mathematical model", Results in Physics **20** (2021) 103676. https://doi.org/10.1016/j.rinp.2020.103676.

[24] N. Faraz, Y. Khan, E. D. Goufo, A. Anjum & A. Anjum, "Dynamic analysis of the mathematical model of COVID-19 with demographic effects", ZeitschriftfürNaturforschung C **75** (2020) 389. https://doi.org/10.1515/znc-2020-0121.

[25] P. Pandey, J. F. Gomez-Aguilar, M. K. Kaabar, Z. Siri & A. M. Allah, "Mathematical modeling of COVID-19 pandemic in India using Caputo-Fabrizio fractional derivative", Computers in biology and medicine **145** (2022) 105518. https://doi.org/10.1016/j.compbiomed.2022.105518.

[26] M. Sivashankar, S. Sabarinathan, V. Govindan, U. Fernandez-Gamiz & S. Noeiaghdam, "Stability analysis of COVID-19 outbreak using Caputo-Fabrizio fractional differential equation", AIMS Mathematics **8** (2023) 2720. https://doi.org/10.3934/math.2023143.

[27] M. A. Dokuyucu & E. Celik, "Analyzing a novel coronavirus model (COVID-19) in the sense of Caputo-Fabrizio fractional operator." Applied and Computational Mathematics, **2021** (2021) 49. https://pesquisa.bvsalud.org/global-literature-on-novel-coronavirus-2019-ncov/resource/pt/covidwho-1220284.

[28] K. Rajagopal, N. Hasanzadeh, F. Parastesh, I. Hamarash, S. Jafari & I. Hussain, "A fractional-order model for the novel coronavirus (COVID-19) outbreak", Nonlinear Dynamics **101** (2020) 11. https://doi.org/10.1007/s11071-020-05757-6.

[29] K. M. Furati, I. O. Sarumi & A. Q. M. Khaliq, "Fractional model for the spread of COVID-19 subject to government intervention and public perception", Applied mathematical modelling **95** (2021) 89. https://doi.org/10.1016/j.apm.2021.02.006.

[30] M. A. Bahloul, A. Chahid & T. M. Laleg-Kirati, "Fractional-order SEIQRDP model for simulating the dynamics of COVID-19 epidemic", IEEE Open Journal of Engineering in Medicine and Biology **1** (2020) 249. https://doi.org/10.1109/OJEMB.2020.3019758.

[31] K. Kozioł, R. Stanisławski & G. Bialic, "Fractional-order SIR epidemic model for transmission prediction of COVID-19 disease", Applied Sciences **10** (2020) 8316. https://doi.org/10.3390/app10238316.

[32] Z. Zhang, A. Zeb, O. F. Egbelowo & V. S. Erturk , "Dynamics of a fractional order mathematical model for COVID-19 epidemic", Advances in Difference Equations **2020** (2020) 1. https://doi.org/10.1186/s13662-020-02873-w.

[33] P. Verma & M. Kumar, "Analysis of a novel coronavirus (2019-nCOV) system with variable Caputo-Fabrizio fractional order",

Chaos, Solitons & Fractals 142 (2021) 110451. https://doi.org/10.1016/j.chaos.2020.110451.

[34] S. Yadav, D. Kumar, J. Singh & D. Baleanu, "Analysis and dynamics of fractional order Covid-19 model with memory effect", Results in Physics **24** (2021) 104017. https://doi.org/10.1016/j.chaos.2021.110859.

[35] D. Denu & S. Kermausuor, "Analysis of a fractional-order COVID-19 epidemic model with lockdown", Vaccines **10** (2022) 1773. https://doi.org/10.3390/vaccines10111773.

[36] M. O. Olayiwola, A. I. Alaje & A. O. Yunus, "A Caputo fractional order financial mathematical model analyzing the impact of an adaptive minimum interest rate and maximum investment demand", Results in Control and Optimization **2023** (2023) 100349. https://doi.org/10.1016/j.rico.2023.100349.

[37] A. I. Alaje, M. O. Olayiwola, K. A. Adedokun, J. A. Adedeji, A. O. Oladapo & Y. O. Akeem, "The modified homotopy perturbation method and its application to the dynamics of price evolution in Caputo-fractional order Black Scholes model", Beni-Suef University Journal of Basic and Applied Sciences **12** (2023) 93. https://doi.org/10.1186/s43088-023-00433-1.

[38] M. O. Olayiwola, A. I. Alaje, A. Y. Olarewaju & K. A. Adedokun, "A Caputo fractional order epidemic model for evaluating the effectiveness of high-risk quarantine and vaccination strategies on the spread of COVID-19", Healthcare Analytics **3** (2023) 100179. https://doi.org/10.1016/j.health.2023.100179.

[39] A. O. Yunus, M. O. Olayiwola, M. A. Omoloye & A. O. Oladapo, "A fractional order model of Lassa disease using the Laplace-Adomian decomposition method", Healthcare Analytics **2023** (2023) 100167. https://doi.org/10.1016/j.health.2023.100167.

[40] M. O. Olayiwola & K. A. Adedokun, "A novel tuberculosis model incorporating a Caputo fractional derivative and treatment effect via the homotopy perturbation method", Bulletin of the National Research Centre **47**(2023) 121. https://doi.org/10.1016/j.health.2023.100167.

[41] M. Ghani, I. Q. Utami, F. W. Triyayuda & M. Afifah, "A fractional SEIQR model on diphtheria disease", Modeling Earth Systems and Environment **9** (2023) 2199. https://doi.org/10.1007/s40808-022-01615-z.

[42] K. Issa, S. A. Olorunnisola, T. Aliu & A. A. Dauda, "Approximate solution of space fractional order diffusion equations by Gegenbauer collocation and compact finite difference scheme: Solution of space fractional diffusion equation", Journal of the Nigerian Society of Physical Sciences **5** (2023) 1368. https://doi.org/10.46481/jnsps.2023.1368.

[43] K. Issa, R. A. Bello & U. J. Abubakar, "Approximate analytical solution of fractional-order generalized integro-differential equations via fractional derivative of shifted Vieta-Lucas polynomial", Journal of the Nigerian Society of Physical Sciences **6** (2024) 1821. https://doi.org/10.46481/jnsps.2024.1821.

[44] O. Nave, U. Shemesh & I. HarTuv, "Applying Laplace Adomian decomposition method (LADM) for solving a model of Covid-19", Computer Methods in Biomechanics and Biomedical Engineering **24** (2021) 1618. https://doi.org/10.1080/10255842.2021.1904399.

[45] A. Ali, V. S. Erturk, A. N. W. A. R. Zeb & R. A. Khan, "Numerical solution of fractional order immunology and AIDS model via Laplace transform Adomian decomposition method", J. Fract. Calcul. Appl. **10** (2019) 242. https://jfca.journals.ekb.eg/article_308514_8f74b43e6193c678bb278bb55de3001e.pdf.

[46] F. Haq, K. Shah, A. Khan & M. Shahzad, "Numerical solution of fractional order epidemic model of a vector-borne disease by Laplace Adomian decomposition method", Punjab University Journal of Mathematics **49** (2020) 13. http://pu.edu.pk/images/journal/maths/PDF/Paper-2_49_2_17.pdf.

[47] A. I. Alaje & M. O. Olayiwola, "A fractional order mathematical model for examining the spatiotemporal spread of COVID-19 in the presence of vaccine distribution", Healthcare Analytics **4** (2023) 100230. https://doi.org/10.1016/j.health.2023.100230.